JOURNAL OF AGRICULTURAL AND FOOD CHEMISTRY

Global Structure of Microwave-Assisted Flash-Extracted Sugar Beet Pectin

MARSHALL L. FISHMAN,*,† HOA K. CHAU,† PETER H. COOKE,§ AND ARLAND T. HOTCHKISS JR.†

Crop Conversion Science and Engineering Research Unit and Microbial Biophysics and Residue Chemistry and Core Technologies Research Unit, Eastern Regional Research Center, Agricultural Research Service, U.S. Department of Agriculture, 600 East Mermaid Lane, Wyndmoor, Pennsylvania 19038

The global structure of microwave-assisted flash-extracted pectins isolated from fresh sugar beet pulp has been studied. The objective was to minimize the disassembly and possibly the degradation of pectin molecules during extraction. These pectins have been characterized by high-performance size exclusion chromatography with light scattering, viscometric detection, and atomic force microscopy (AFM). Analysis of molecular parameters was performed on 15 and 8 μm size column packings. Samples analyzed with 15 μm packing gave weight-average molar masses that ranged from 532,000 to 1.2 million Da, radii of gyration from about 35 to 51 nm, polydispersities from 1.78 to 2.58, intrinsic viscosities from about 3.00 to 4.30 dL/g, and recoveries from 8.40 to 14.81% of dry weight. Chromatography revealed that a bimodal distribution of high molar mass spherical particles and lower molar mass coils was obtained. AFM images of pectin corroborated this conclusion and further revealed that these strands and spherical particles were integrated into networks. It is demonstrated that microwave-assisted extraction of sugar beet pulp under moderate pressure and at relatively low temperature could extract under acid conditions high molar mass, moderate-viscosity pectin in minutes rather than hours as required by conventional heating.

KEYWORDS: Sugar beet pulp; microwave heating; HPSEC; molar mass; intrinsic viscosity; radius of gyration; atomic force microscopy

INTRODUCTION

It is estimated that about 2 million tons of dry sugar beet pulp is generated annually by U.S. industry as a result of the extraction of sugar from sugar beet (*1*). This residue is utilized mainly as low-value animal feed. The high cost of energy required to dry SBP and worldwide increases in agricultural production, which produces other residues capable of being used as animal feed, threatens to diminish the market for sugar beet pulp as animal feed. In addition, diminished use of SBP as animal feed would require that the pulp be disposed of in an environmentally acceptable manner, which could add to the cost of producing sugar.

About 67% of SBP on a dry weight basis is composed of plant cell wall polysaccharides. About 19% of these polysaccharides are pectin, 21% pectin-associated arabinan, and 24% cellulose (*2*). All of these potentially could add value to SBP if isolated and their functional properties characterized. In this research, we have focused on the isolation and characterization of high molar mass pectin.

Pectins are polysaccharides in which (1→4)-linked α-D-galacturonates and their methyl esters predominate (*1*). In addition to these "smooth" homogalaturonan (HG) regions, also common to all pectins are "hairy" regions, which are composed of rhamnogalacturonan (RG) units (*3*). HG and RG galacturonic acid OH protons may be substituted with acetyl groups, whereas those protons in HG also can be substituted with xylose. The (1→2)-linked rhamnose units in the RG region may be substituted with galactan, arabinan, or arabinogalactan side chains in the 4-position.

Pectin from sugar beets often differs from other sources of pectin in that it tends to have a higher degree of acetylation and a higher neutral sugar content (*4*). Furthermore, unlike pectins from many other sources, sugar beet pectin contains feruloyl groups (*4*). Moreover, unlike pectin from citrus peels or apple pomace, sugar beet pectin does not gel when high concentrations of sugar under acid conditions are present. The poor gelling properties of sugar beet pectin have been attributed to the presence of acetyl groups and relatively low molar mass (*5, 6*). It also has been suggested that the relatively high

* Author to whom correspondence should be addressed [telephone (215) 233-6450; fax (215) 233-6406; e-mail marshall.fishman@ars.usda.gov].

† Crop Conversion Science and Engineering Research Unit.

§ Microbial Biophysics and Residue Chemistry and Core Technologies Research Unit.

10.1021/jf072600o This article not subject to U.S. Copyright. Published 2008 by the American Chemical Society
Published on Web 01/10/2008

amounts of neutral sugar side chains in sugar beet pectin prevent it from gelling (*7*).

There have been numerous studies on the structural characteristics and physicochemical properties of pectin from sugar beet pulp (*8*). Also, there have been many studies involving the structural characteristics and physicochemical properties of enzymatically and chemically modified sugar beet pectins from pulp (*9*). Most of these studies were concerned with the fine structure of sugar beet pectin and how it might affect its functional properties. Few if any of these studies were directed toward understanding the global structure of sugar beet pectin.

Recently, sugar beet pectin extracted by acid from cell walls isolated from fresh sugar beet roots and characterized by atomic force microscopy (AFM) revealed linear and branched molecules attached to globular molecules (*10*). The linear molecules were attributed to polysaccharides, whereas the globular particles were attributed to proteins. Furthermore, others have shown that the physical properties of pectin are highly dependent on the conditions of extraction (*7*).

In this research we have studied the global structure of microwave-assisted flash-extracted pectins isolated from fresh sugar beet pulp. The intention was to minimize the disassembly and possibly the degradation of pectin molecules during extraction. We have characterized the flash-extracted pectins by HPSEC with light scattering and viscometric detection and also by AFM.

MATERIALS AND METHODS

Sugar Beet Pulp. Partially dewatered SBP with sugar removed was a gift from American Crystal Sugar, Moorehead, MN. SBP was shipped frozen and stored at −20 °C until prepared for extraction. The frozen sample was dried by Dryer shelf Vac (New York Engineering Co., Yonkers, NY) and ground by a Wiley Mill no. 1 (Arthur H. Thomas Co) to approximately 20 mesh.

Microwave-Assisted Extraction (MAE). The extraction method has been described elsewhere with some modification (*11, 12*). Briefly, microwave heating was performed in a CEM Corp. model Mars X microwave sample preparation system equipped with valves and tubing, which permitted the application of external pressure to each of the extraction vessels via nitrogen from a tank equipped with a pressure gauge. Samples were irradiated with 1200 W of microwave power at a frequency of 2450 MHz. One gram of ground sugar beet pulp was dissolved in 20 mL of pH 1.0 HCl and stirred at room temperature for 2 h, after which 5 mL more of pH 1 acid was added. For each experiment, vessels interconnected with tubing were placed in the sample holder, a rotating carousel. One vessel was equipped with temperature and pressure sensors that measured/controlled the temperature and pressure within the cell. After heating, the samples were allowed to cool in a water bath for 0.5 h at room temperature and filtered through miracloth. The filtrate was precipitated with a 2:1 ratio of 95% IPA in water. The samples were vaccuum-dried at room temperature and stored under vacuum until analyzed.

Chromatography. Dry sample (2 or 4 mg/mL) was dissolved in mobile phase (0.05 M $NaNO_3$), centrifuged at 50000*g* for 10 min, and filtered through a 0.22 or 0.45 μm Millex HV filter (Millipore Corp., Bedford, MA). The flow rate for the solvent delivery system, a model 1100 series degasser, autosampler, and pump (Hewlett-Packard Corp.), was set at 0.7 mL/min. The injection volume was 200 μL. Samples were run in triplicate. The column set consisted of two PL Aquagel OH-60 and one OH-40 size exclusion column (Polymer Laboratories, Amherst, MA) in series. During the course of the research, samples were analyzed using column sets with 8 and 15 μm particle size column packings, respectively. The columns were in a water bath set at 35 °C. Column effluent was detected with a Dawn DSP multiangle laser light scattering photometer (MALLS) (Wyatt Technology, Santa Barbara, CA), in series with a model H502 C differential pressure viscometer (DPV) (Viscotek Corp., Houston, TX) and an Optilab DSP interferometer (RI) (Wyatt Technology). Electronic outputs from the 90° light scattering angle, DPV, and RI were sent to one directory of a personal computer for processing with TRISEC software (Viscotek Corp.). Electronic outputs from all of the scattering angles measured by the MALLS, DVP, and RI were sent to a second directory for processing with ASTRA software (Wyatt Technology).

Atomic Force Microscopy. For solution studies, sugar beet pectin sample 3/60/30 (time/temperature/pressure) was dissolved in HPLC grade water and serially diluted to the desired concentration. Two microliters of the solution was pipetted onto a freshly cleaved 10 mm diameter disk of mica and air-dried. The mica was mounted in a Multimode Scanning Probe microscope with a Nanoscope IIIa controller, operated as an atomic force microscope in the tapping mode (Veeco Instruments, Santa Barbara, CA). The thin layer of pectin adhering to the mica surface was scanned with the atomic force microscope operating in the intermittent contact mode using etched silicon probes (TESP). The spring constants for these probes were 20–100 N/m, and the nominal tip radius of curvature was 5–10 nm (*13*). The cantilever controls, namely, drive frequency, amplitude, gains, and amplitude set point ratio (rsp), were adjusted to give images with the clearest image details. Values of rsp used in this study were about 0.95. The definition of rsp is given by eq 1:

$$\text{rsp} = \text{Asp/Ao} \quad (1)$$

Asp is the oscillating amplitude in contact with the sample, whereas Ao is the freely oscillating amplitude (out of contact amplitude). Set point amplitudes approaching 1 correspond to light normal forces, that is, soft tapping (*14*).

Images were analyzed by software version 5.12 rev. B, which is described in the Command Reference Manual supplied by the manufacturer. Heights and diameters of spherical particles were determined by particle analysis. For individual molecules in dilute solution this process is straightforward. In the case of network's objects of interest (OOI), the OOI must be separated from other objects by a process called threshold segmentation. To accomplish this we chose a threshold value for pixel intensity, which removed or masked the intensity of background pixels and allowed the pixel brightness of OOIs to remain essentially undiminished. Prior to particle analysis, low pass filtering was applied to reduce background noise and high pass filtering was applied to highlight the OOI, which are delineated from the background as areas of rapidly changing height or phase. Height images were acquired as 1.0 or 2.5 μm wide fields at 512 × 512 pixel resolution. Height images were planefit (auto *X* and *Y* axes) and flattened, and contrast in color (**Table 2**) was adjusted to compare visually with the *z* scale (height) setting.

Compositional Analysis. Anhydrogalacturonate content (% AGA) was determined by using the sulfamate/3-phenylphenol colorimetric method (*15*) as modified by Yoo et al. (*16*). Degree of methyl esterification (% DM) and acetylation (% DA) were determined by HPLC (*17*). Neutral sugar content (% NS) was determined with the phenol−sulfuric acid colorimetric method (*18*). Percentage of alcohol-insoluble pectin was determined gravimetrically (% PR). The protein content of pectin was estimated using standard methods for determining the nitrogen content of samples by use of a combustion instrument followed by thermal conductivity (*19, 20*). A Flash EA 1112 elemental analyzer (CE Elantech, Inc., Lakewood, NJ) calibrated with aspartic acid was used for the nitrogen determination. Percentage nitrogen was multiplied by 6.25 to obtain an estimation of protein (*21*).

Statistical Analysis. In each table, data were analyzed by analysis of variance to test the effect of the treatments under study. Mean separations were performed using the Bonferroni LSD separation technique at the $p = 0.05$ level.

RESULTS AND DISCUSSION

Microwave Assisted Extraction. Previously (*12, 22–24*) we have shown that MAE under pressure produced pectin from the peels of limes and oranges with higher molar mass and viscosity and significantly shorter heating times than pectin extracted with conventional heating. In view of the structural (*25, 26*)and chemical (*7*) complexity of pectins, we employed MAE of sugar beet pulp with the expectation that sugar beet pectin (SBP) would

Table 1. Compositional Analysis of Sugar Beet Pectin Extracted at 60 °C

time (min)/pressure (psi)	recovered	% AGA	% NS	% DM	% DA	% protein[a]
commercial		57.0 (0.8)	38.5 (1.7)	82.9 (9.3)		5.59 (0.2)
3/25	12.99	51.8 (2.6)[b]	40.8 (1.1)	99.0 (5.7)	58.7 (3.5)	
3/30	11.25	48.3 (2.3)	44.7 (3.5)	113.3 (13.0)	67.6 (5.0)	8.56 (0.02)
3/75	9.23	60.3 (2.9)	29.1 (3.2)	77.4 (4.2)	43.6 (2.3)	
5/50	8.91	52.6 (1.7)	36.4 (4.5)	101.8 (4.3)	57.1 (2.2)	
5/75	10.43	53.7 (1.6)	26.9 (1.7)	103.8 (6.6)	55.3 (3.5)	
10/25	11.88	52.7 (2.5)	30.2 (1.9)	103.0 (5.9)	60.3 (3.2)	
10/30	10.34	53.9 (3.9)	33.0 (2.1)	86.1 (7.9)	43.1 (5.0)	
10/50	16.80	66.5 (2.1)	12.6 (1.5)	71.5 (3.6)	36.7 (1.6)	
10/75	11.30	57.6 (1.8)	33.7 (3.5)	83.2 (3.2)	49.0 (1.8)	
15/50	14.81	54.7 (3.0)	34.9 (3.7)	93.7 (8.5)	56.3 (4.6)	
20/50	11.34	51.5 (1.9)	29.3 (2.2)	109.6 (6.6)	63.8 (3.5)	
av[c]	11.8 (2.5)	54.9 (5.0)	32.0 (8.3)	94.8 (13.5)	53.8 (9.5)	

[a] Determined by multiplying Kjehldahl nitrogen by 6.25. [b] Standard deviation of triplicate analyses. [c] Does not include commercial sample.

Table 2. Weight-Average Molar Mass ($M_w \times 10^{-3}$) of Pectin

time/temp/pressure (min, °C, psi)	2 mg/mL[a], MALLS[c]	8 μm[b], LS/V[d]	2 mg/mL, MALLS	15 μm, LS/V	4 mg/mL, MALLS	8 μm, LS/V
3/60/19	815 (1)[e]	939 (3)	956 (5)	1180 (20)		
3/60/23	1070 (10)	1330 (6)	978 (3)	1150 (6)		
3/60/25			1020 (70)	1250 (20)	907 (20)	1240 (40)
3/60/30	807 (57)	683 (73)	1200 (6)	1520 (10)	1080 (6)	1490 (20)
3/60/50			622 (3)	641 (5)		
3/60/60			517 (7)	518 (10)		
3/60/75	570 (9)	765 (5)	753 (8)	852 (7)	570 (9)	616 (4)
3/70/30	772 (20)	862 (20)	781 (5)	878 (7)	739 (6)	935 (4)
5/60/50	690 (5)	835 (2)	743 (10)	768 (30)	690 (5)	763 (10)
5/60/75	745 (8)	790 (7)	751 (3)	782 (3)	763 (5)	991 (2)
10/50/50	802 (5)	961 (5)	854 (10)	832 (1)	933 (5)	1240 (20)
10/50/75	839 (2)	1020 (6)	839 (10)	1010 (6)	894 (2)	1140 (10)
10/60/25	746 (4)	858 (10)	895 (2)	1090 (6)	823 (2)	965 (2)
10/60/30	782 (2)	866 (5)	818 (7)	967 (20)	770 (6)	912 (3)
10/60/40			681 (10)	774 (30)		
10/60/50	888 (9)	1070 (0)	966 (3)	1020 (10)	868 (4)	1090 (10)
10/60/60			600 (8)	645 (6)		
10/60/75			970 (4)	1190 (6)		
10/70/50	855 (3)	1020 (10)	932 (3)	1100 (10)	894 (2)	1070 (1)
10/70/75	790 (4)	909 (5)	758 (4)	883 (1)	833 (2)	1060 (1)
10/45/60			522 (5)	548 (9)		
15/60/50	849 (9)	940 (1)	1030 (10)	1190 (20)	873 (2)	1140 (10)
20/60/50	791 (10)	917 (2)	872 (1)	1010 (1)	824 (4)	977 (6)

[a] Injected concentration. [b] Particle size of column packing. [c] Multiangle laser light scattering method. [d] Light scattering, viscosity detection method. [e] Standard deviation of triplicate analysis.

undergo minimal degradation. The ultimate goal is to assess the properties of SBP for value-added applications. Typically, SBP is extracted at temperatures ranging from 75 to 95 °C and times between 30 and 90 min. With the aid of MAE, we have extracted SBP at times ranging from 3 to 20 min, temperatures between 45 and 70 °C, and pressures between 19 and 75 lb/in.^{2}. **Figure 1** is a plot of pressure and temperature against time for SBP extracted by microwave heating. In that experiment, the sample reached the desired temperature (ca. 60 °C) and pressure (ca. 30 lb/in.^{2}) in a little more than 1 min. The pressure is applied from an external source because the temperature is below 100 °C.

Compositional Analysis. Table 1 contains percentages of pectin recovered (% PR), anhydrogalacturanate (% AGA), neutral sugars (% NS), degree of methylesterification (% DM), and degree of acetylization (% DA) for microwave extractions at 60 °C. Heating times ranged from 3 to 20 min and pressures from 25 to 75 lb/in.^{2}. Although there was some evidence for differences between the various time/pressure combinations, there appeared to be little correlation between time or pressure with percentage of PR, AGA, NS, DM, and DA. Therefore, compositional and recovery values were averaged without regard to time or pressure. Average % PR was 11.8 ± 2.4, % AGA was 54.9 ± 5.0, % NS was 32.0 ± 8.3, % DM was 94.8 ± 13.5, and % DA was 53.8 ± 9.5. By way of comparison (*7*) for fresh sugar beets extracted at pH 1 and 75 °C for 30 min with

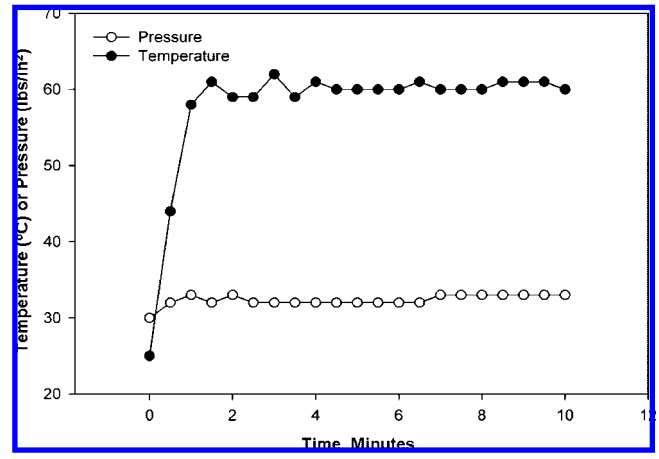

Figure 1. Typical pressure and temperature curve as a function of heating time for the microwave-assisted extraction of pectin from sugar beet pulp.

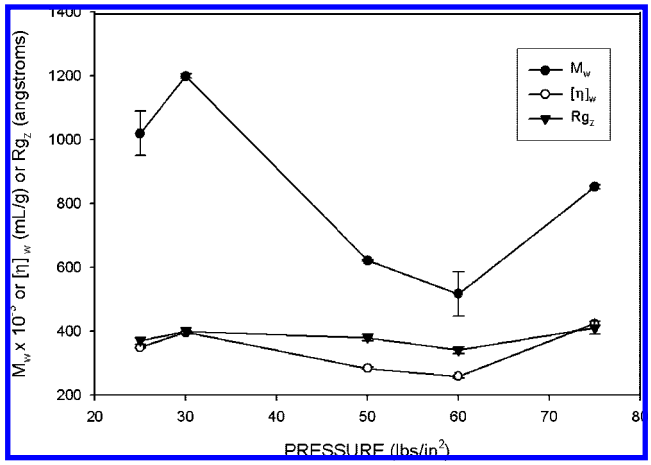

Figure 2. Effect of pressure on weight-average molar mass (M_w), weight-average intrinsic viscosity ($[\eta_w]$), and *z*-average radius of gyration ($R_{g,z}$) on sugar beet pectin. Heating time was 3 min. Final temperature was 60 °C.

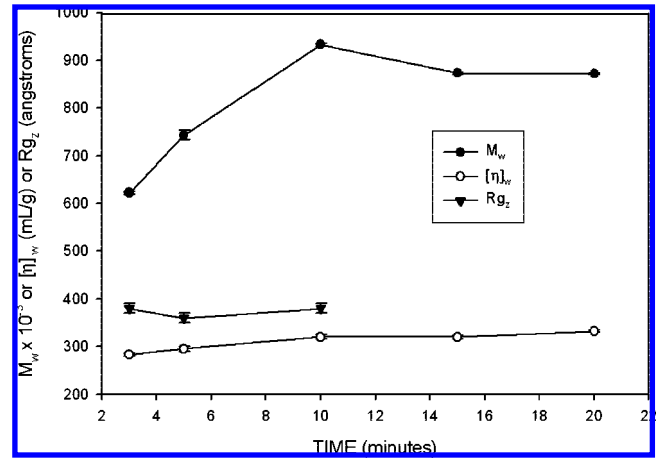

Figure 3. Effect of heating time on weight-average molar mass (M_w), weight-average intrinsic viscosity ($[\eta_w]$), and *z*-average radius of gyration ($R_{g,z}$) on sugar beet pectin. Pressure was 50 lb/in.^{2}. Final temperature was 60 °C.

HCl, % PR was 32.9, % AGA was 38.0, % NS was 37.1, % DM was 54, and % DA was 28. Thus, % PR and % NS were lower for fresh sugar beet pulp heated by microwaves when compared to conventionally heated fresh sugar beets, whereas % AGA, % DM, and % DA were higher. Comparisons between the 3/60/30 and the commercial samples revealed that the percentage of AGA was higher for the commercial sample but the percentages of NS and DM were lower, which may indicate that the commercial sample underwent greater degradation of neutral sugar side chains and possibly more deesterification. Furthermore, comparison revealed that the crude protein content of the 3/60/30 sample was 8.56 ± 0.02%, whereas that of the commercial sample was 5.59 ± 0.2%. The difference in protein content between the two samples was statistically significant.

Molar Mass, Radius of Gyration, and Intrinsic Viscosity. The data in **Table 2** reveal that the molar mass was higher when LS/V (triple detector) rather than when the MALLS method of detection and characterization was used. There was no evidence of significant differences in molar mass due to particle size or injected concentration. In **Figure 2**, we have plotted the effect of pressure on molecular properties when the sugar beet pulp was heated for 3 min with a final temperature of 60 °C. Whereas the molar mass of the extracted pectin varied with pressure, intrinsic viscosity and radius of gyration were relatively constant. Molar mass reached a maximum at 30 lb/in.^{2}. Thereafter, molar mass decreased with increasing pressure until 60 lb/in.^{2}, at which pressure it started to increase. These changes in molar mass with pressure may be indicative of the heterogeneity of sugar beet pectin within the cell wall. Changes in molar mass of sugar beet pectin at relatively constant intrinsic viscosity and radius of gyration could be rationalized if the pectin was composed of spherically shaped molecules with a distribution of packing densities. The rise in molar mass between 60 and 70 lb/in.^{2} could signify the release of pectin from a different section of the cell wall.

The effect of heating time at 60 °C and 50 lb/in.^{2} on the molecular properties of sugar beet pectin (see **Figure 3**) again shows the molar mass may change while intrinsic viscosity and radius of gyration remain relatively constant. **Table 3** contains the molecular properties of pectins analyzed by columns with 15 μm size particles. Weight-average molar mass (M_w) ranged from 532,000 to 1.2 million Da, *z*-average root-mean-square radius of gyration ($R_{g,z}$) ranged from about 35 to 51 nm, and the weight-average intrinsic viscosity ($[\eta_w]$) ranged from about 3.00 to 4.30 dL/g. There was evidence of significantly greater values for M_w and $[\eta_w]$ in the 3/60/30 sample when compared to the commercial sample. There was no evidence for differences in $R_{g,z}$. This could occur for two samples that have the same average size but different compositions with respect to the shape of constituent molecules.

Table 3. Molecular Properties of Pectin from Sugar Beet[a]

time/temp/pressure (min, °C, psi)	$M_w \times 10^{-3}$	$R_{g,z}$ (nm)	$[\eta_w]$ (dL/g)
commercial	640 (14)	40.4 (2)	3.27 (0.03)
3/60/19	956 (5)	40.1 (0.3)	4.23 (0.05)
3/60/23	978 (3)	35.2 (0.5)	3.81 (0.06)
3/60/25	1020 (70)	37.3 (1)	3.49 (0.08)
3/60/30	1200 (6)	40.3 (0.3)	3.97 (0.02)
3/60/50	622 (3)	37.6 (1)	2.83 (0.03)
3/60/60	517 (7)	34.3 (0.4)	2.58 (0.05)
3/60/75	753 (8)	40.8 (2)	4.24 (0.07)
3/70/30	781 (5)	36.3 (0.5)	3.45 (0.03)
5/60/50	743 (10)	36.4 (0.2)	2.95 (0.05)
5/60/75	751 (3)	45.3 (0.5)	3.75 (0.05)
10/50/50	854 (10)	50.5 (2)	4.11 (0.02)
10/50/75	839 (10)	38.5 (1)	3.76 (0.02)
10/60/25	895 (2)	38.1 (0.2)	3.74 (0.01)
10/60/30	818 (7)	39.1 (0.7)	4.14 (0.06)
10/60/40	681 (10)	33.9 (2)	3.43 (0.1)
10/60/50	966 (3)	38.2 (2)	3.20 (0.05)
10/60/60	600 (8)	32.9 (0.5)	3.58 (0.1)
10/60/75	970 (4)	38.4 (0.5)	3.70 (0.02)
10/70/50	932 (3)	38.8 (0.7)	3.66 (0.02)
10/70/75	758 (4)	40.4 (1)	3.69 (0.04)
10/45/60	522 (5)	34.7 (1)	3.04 (0.1)
15/60/50	1030 (10)	35.4 (0.4)	3.20 (0.04)
20/60/50	872 (1)	34.9 (0.3)	3.32 (0.02)

[a] Sample concentration, 2 mg/ml; column packing size, 15 μm.

Superimposed light scattering (LS), viscosity (DP), and refractive index (RI) chromatograms of pectin heated during extraction for 3 min at 60 °C under a pressure of 30 lb/in.^{2} plotted against retention volume are shown in **Figure 4**. The separation of the LS chromatogram from the DP and RI chromatograms, which have a high degree of overlap, could indicate the presence of a continuum of compact high molar mass fractions which transition into lower molar mass fractions that are less compact. We have plotted the integral and differential distribution curves in **Figure 5**. The differential distribution curve clearly shows that the distribution is bimodal.

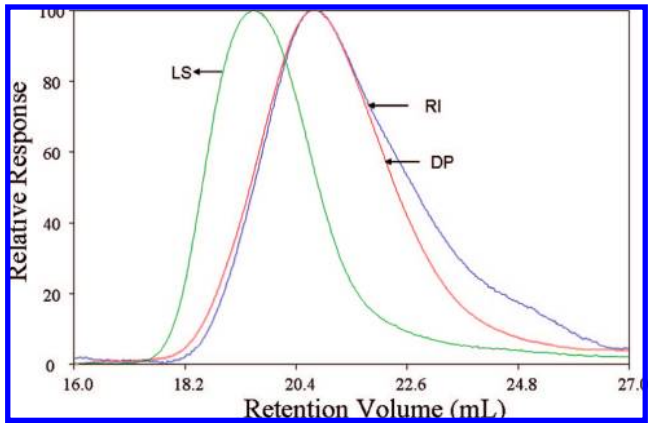

Figure 4. Superimposed light scattering (LS), viscosity (DP), and refractive index (RI) chromatograms of pectin. Heating time was 3 min. Temperature was 60 °C. Pressure was 30 lb/in.^{2}.

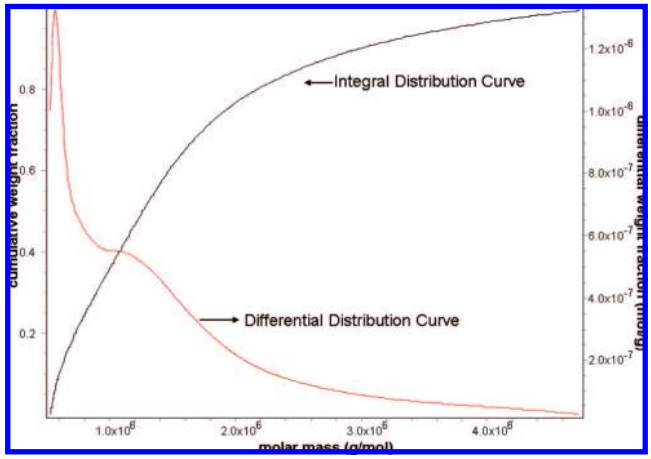

Figure 5. Distribution analysis of sugar beet pectin molar masses. Heating time was 3 min. Temperature was 60 °C. Pressure was 30 lb/in.^{2}.

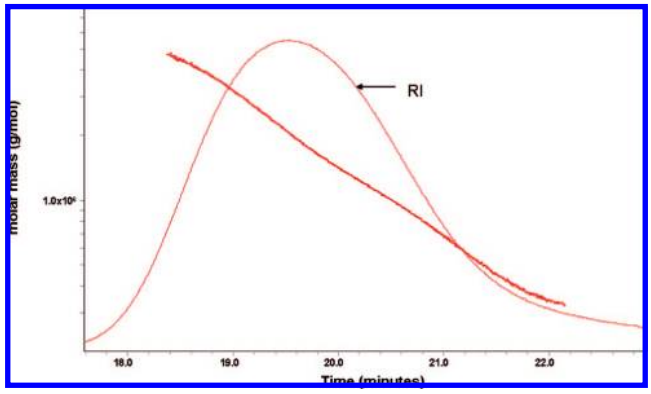

Figure 6. HPSEC molar mass calibration curve for sugar beet pectin superimposed on refractive index (RI) chromatogram. Heating time was 3 min. Temperature was 60 °C. Pressure was 30 lb/in.^{2}.

In **Figures 6** and **7** are HPSEC molar mass and radius of gyration calibration curves, respectively, constructed from the pectin sample heated during extraction for 3 min at 60 °C under a pressure of 30 lb/in.^{2}. Both calibration curves are superimposed on the RI chromatogram. The gradual changes in slope of the calibration curves in both figures indicate a continuous change in molar mass and radius of gyration as the elution of molecules from the column progresses from higher to lower molar mass and size. In the case of the R_g curve, the upturn at elution times between 21 and 22 min is due to poor sensitivity of the LS instrument to measure radii below 30 nm for this sample.

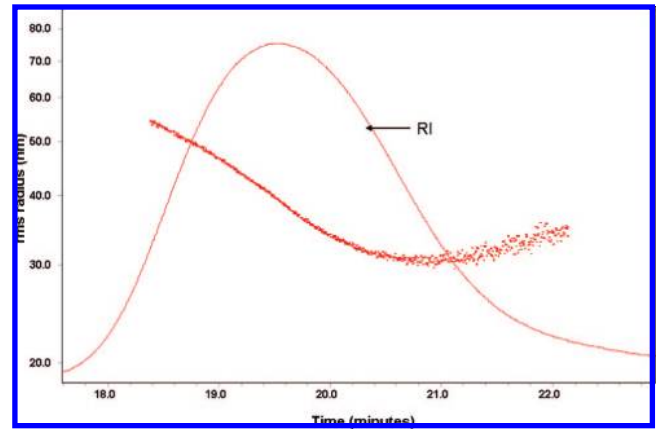

Figure 7. HPSEC radius of gyration calibration curve for sugar beet pectin superimposed on refractive index (RI) chromatogram. Heating time was 3 min. Temperature was 60 °C. Pressure was 30 lb/in.^{2}.

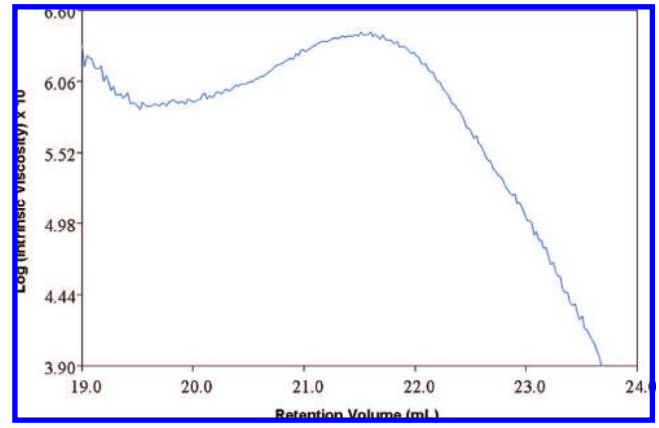

Figure 8. Log intrinsic viscosity against retention volume for sugar beet pectin. Heating time was 3 min. Temperature was 60 °C. Pressure was 30 lb/in.^{2}.

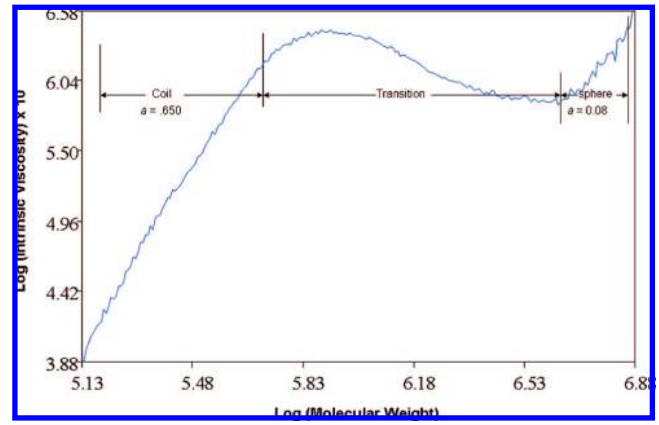

Figure 9. Mark–Houwink plot for sugar beet pectin. Heating time was 3 min. Temperature was 60 °C. Pressure was 30 lb/in.^{2}.

In contrast to the curves in **Figures 6** and **7**, the intrinsic viscosity calibration curve for the 3 min sample is not well behaved (see **Figure 8**). The curve in **Figure 8** passes through a minimum followed by a maximum at longer elution times. We have plotted log intrinsic viscosity against log molar mass in **Figure 9**, the Mark–Houwink (M−H) plot. The shape of this plot is comparable to the plot in **Figure 8** except that the molar mass increases from left to right rather than from right to left. The plot has been divided into three regimes as marked by four vertical lines with the values of "*a*", the slope or Mark–Houwink

Table 4. Molecular Properties of Sugar Beet Pectin Fractions[a]

fraction	% recovery	$M_w \times 10^{-3}$	$[\eta]_w$ (dL/g)	$R_{g,z}$ (nm)	a^b
1, sphere[c]	7.8 (0.6)[d]	3724 (154)	3.83 (0.07)	54.1 (1.0)	0.076 (0.02)
2, transition	59.5 (1)	1319 (37)	4.12 (0.02)	39.1 (0.3)	
3, random coil[c]	34.0 (1)	394 (8)	3.71 (0.04)	37.6 (0.4)	0.650 (0.06)

[a] 3/60/30, time (min)/temperature (°C)/pressure (psi). [b] Mark–Houwink exponent. [c] Determined from "*a*". [d] Standard deviation (triplicate analyses).

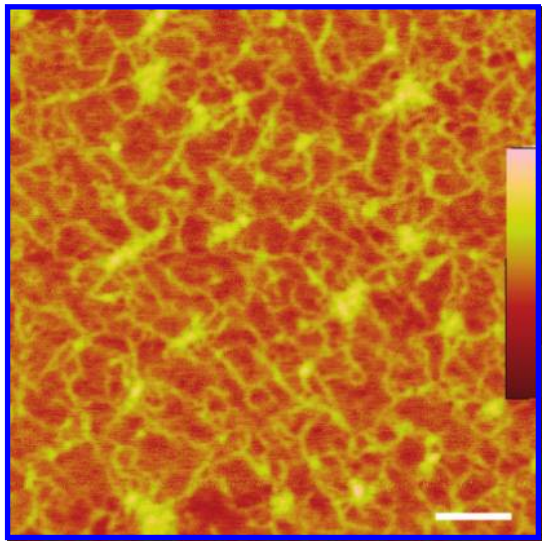

Figure 10. AFM image of sugar beet pectin network deposited from water at a concentration of 12.5 μg/mL. Scale bar is 100 nm; inset height scale is 0–2.5 nm.

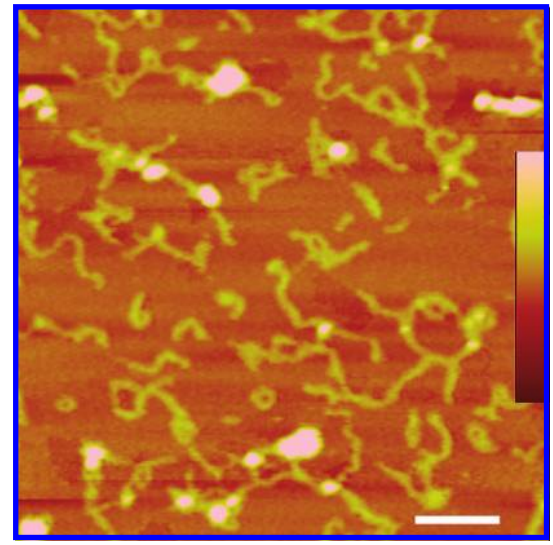

Figure 11. AFM image of sugar beet pectin, dissociated at a concentration of 6.25 μg/mL. Scale bar is 100 nm; inset height scale is 0–5 nm.

exponent, indicated for each section of the plot. The molecular properties for these three regimes are given in **Table 4**. The high molar mass regime had an M−H exponent of 0.076, which indicates an extremely compact molecule. This regime comprised about 7.8% of the weight of the sample. The low molar mass regime comprised about 34% of the weight of the sample and had an M−H exponent of 0.65, which indicated a much less compact molecule than the high molar mass fraction. The intermediate or overlap regime is a transition region in which both high and low molar mass fractions may coexist. The transition regime has both M_w and $R_{g,z}$ values that fall between the values for the high and low fractions. The values of $[\eta_w]$ for the high and low molar mass regimes are not significantly different but, interestingly, are different from the transition region.

In an effort to further elucidate its structure, images of sugar beet pectin were obtained by AFM. The sugar beet pectin was deposited onto mica from dilute water solution and air-dried. In **Figure 10** is an image of a sugar beet pectin network obtained by depositing a 2 μL drop of pectin dissolved in water at a concentration of 12.5 μg/mL. The image revealed a number of spherical or odd-shaped particles surrounded by strands. Many of the particles appear to be in contact with multiple strands, thus appearing to be embedded in an open network structure. Dilution of the sugar beet pectin in water to 6.25 μg/mL produced the image in **Figure 11**. In that figure the network has fragmented into particles attached to expanded strands. The strands appear to be composed of rods, kinked rods, and segmented rods. Many of these appear to be aggregated end to end and/or side by side. Some of the strands have formed closed loops. The images in **Figure 11** appear to be similar to peach pectin networks fragmented by dissolution in 5 mm NaCl and imaged by electron microscopy (*25, 26*). Nonetheless, spherical or odd-shaped particles were not observed in the peach pectin images.

Table 5. Molecular Dimensions of Spherical Sugar Beet Pectin Particles

concn (μg/mL)	height[a] (nm)	height sigma[b] (nm)	diameter (nm)	diameter sigma (nm)
12.5	0.50 (0.04)[c]	0.28 (0.06)	12.3 (1.6)	12.3 (1)
6.25	0.77 (0.03)	0.41 (0.06)	15.2 (0.8)	10.3 (0.7)

[a] Mean. [b] One sigma breadth of the entire field. [c] Standard deviation of three measurements.

Table 6. Molecular Dimensions of Spherical Sugar Beet Pectin Particles

concn (μg/mL)	height[a] (nm)	height sigma[b] (nm)	diameter (nm)	diameter sigma (nm)
12.5	0.9 (0.2)[c]	0.35 (0.07)	28.3 (4.2)	10.5 (2.9)
6.25	1.3 (0.1)	0.72 (0.12)	30.6 (2.5)	10.6 (2.0)

[a] Mean. [b] One sigma breadth of the dimension distributions for 50 of the largest particles. [c] Standard deviation of three measurements.

Table 7. Molecular Dimensions of a Single Spherical Sugar Beet Pectin Particle

concn (μg/mL)	height[a] (nm)	diameter (nm)
12.5	0.51 (0.06)[b]	20.2 (4.0)
6.25	0.75 (0.04)	17.7 (2)

[a] Mean. [b] Standard deviation of three measurements.

In **Tables 5** and **6** we compare the height and diameter of the spherical portions of the networks after segmentation analysis for an entire field and for 50 of the largest particles, respectively. Segmentation analysis essentially removes the strands of the networks from the image. In both tables, there appears to be no difference in diameter size at the two concentrations, whereas heights appear to be significantly higher at 6.25 μg/mL than at 12.5 μg/mL. These differences may be due to increased charge–charge repulsions, which can occur simultaneously with

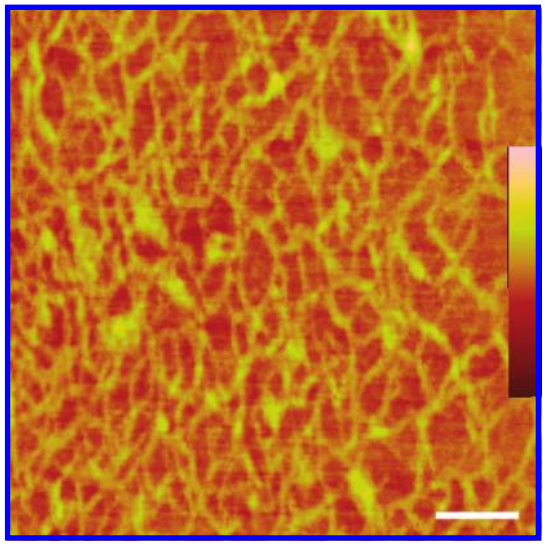

Figure 12. AFM image of orange pectin network, deposited from water at a concentration of 13.1 μg/mL. Scale bar is 100 nm; inset height scale is 0–4 nm.

pectin dissociation at the lower concentration (*27*). Nonetheless, the radii of the compact particles measured by AFM are about a factor of 5 or more times smaller than the $R_{g,z}$ measured by light scattering; compare values of $R_{g,z}$ in **Table 4** for a sphere with half the diameter of values found in **Tables 5** and **6**. From three spherical particles obtained after segmentation analysis from particles shown in **Figure 11**, we chose a particle from each of three fields for which the collective average height was 0.76 ± 0.04 nm and the average diameter, 18 ± 2 nm. Half of this value, 9 nm, also is significantly smaller than the radius of the spheres measured in solution, which was 54 ± 1 nm. Because molecules measured by HPSEC are about 10−20 times more concentrated than those measured by AFM, the molecules measured by HPSEC are probably more aggregated. Furthermore, the greater size of radii dimensions from HPSEC measurements as compared to measurements from AFM may be due to larger charge–charge repulsions in the hydrated pectin from HPSEC measurements as compared to air-dried pectin imaged by AFM.

Nonetheless, pectin imaged in **Figure 10**, which was deposited from solution at a concentration of 12.5 μg/mL, forms loose networks that extend over areas in excess of 1^2 μm. In this case even though the pectin concentration was appreciably lower than the concentration used in HPSEC experiments, it was sufficiently high in the absence of added salt to allow weak networks to form, which were held together by secondary forces and which were larger than the aggregates determined in the solution study.

Figure 12 is an AFM image of pectin extracted from orange albedo. The orange pectin was dissolved in water at a concentration 13.1 μg/mL prior to deposition on mica, whereas the concentration of sugar beet pectin was 12.5 μg/mL. The origin and extraction of the orange pectin have been described previously (*27*). Comparison of the sugar beet image in **Figure 10** with the orange pectin image in **Figure 12** reveals that the sugar beet pectin network is somewhat more open than the orange pectin network. Unlike peach pectin images, spherical particles appear in both images, but those in the orange pectin image appear to be fewer in number than those in the sugar beet pectin image.

In conclusion, we have demonstrated that MAE of sugar beet pulp under moderate pressure and at relatively low temperature could extract under acid conditions high molar mass, moderate-viscosity pectin in minutes rather than hours as required by conventional heating. HPSEC with online light scattering and viscosity detection revealed that a bimodal distribution of high molar mass spherical particles and lower molar mass coils was obtained. AFM images of air-dried solutions of sugar beet pectin corroborated this conclusion and further revealed that these strands and spherical particles were integrated into networks. Comparison of AFM images of sugar beet pectin and orange pectin revealed that sugar beet produced more spherical particles but the networks were somewhat more open.

ACKNOWLEDGMENT

We thank André White for technical assistance in determining compositional analysis of sugar beet pectin carbohydrates, Robyn Moten and Michael Kurantz for assistance in determining protein composition, Halla Sulleiman for technical assistance in processing AFM data, and John Phillips for assistance in performing statistical analysis.

LITERATURE CITED

(1) http://bioweb.sungrant.org (search for sugar beets).
(2) Oosterveld, A.; Beldman, G.; Schols, Henk, A.; Voragen, A. G. J. Arabinose and ferulic acid rich pectic polysaccharides extracted from sugar beet pulp. *Carbohydr. Res.* **1996**, *288*, 143–153.
(3) Carpita, N.; McCann, M. C. The cell wall. In *Biochemistry and Molecular Biology of Plants*; Buchanan, B., Ed.; American Society of Plant Physiologists: Rockville, MD, 2000; pp 52–108.
(4) Rombouts, F. M.; Thibault, J.-F. Feruloylated pectic substances from sugar beet pulp. *Carbohydr. Res.* **1986**, *154*, 177–187.
(5) Roboz, E.; Van Hook, A. Chemical study of beet pectin. *Proc. Am. Soc. Sugar Beet Technol.* **1946**, *4*, 574–583.
(6) Pippen, E. L.; McCready, R. M.; Owens, H. S. Gelation properties of partially acetylated pectins. *J. Am. Chem. Soc.* **1950**, *72*, 813–816.
(7) Levigne, S.; Ralet, M.-C.; Thibault, J.-F. Characterization of pectins extracted from fresh sugar beet under different conditions using an experimental design. *Carbohydr. Polym.* **2002**, *49*, 145–153.
(8) Oosterveld, A.; Beldman, G.; Voragen, A. G. J. Enzymatic modification of pectic polysaccharides obtained from sugar beet pulp. *Carbohydr. Polym.* **2002**, *48*, 73–81.
(9) Bucholt, H. C.; Christensen, T. M. I. E.; Fallensen, B.; Ralet, M.-C.; Thibault, J.-F. Preparation and properties of enzymatically and chemically modified sugar beet pectins. *Carbohydr. Polym.* **2004**, *58*, 149–161.
(10) Kirby, A. R.; MacDougall, A. J.; Morris, V. J. Sugar beet−protein complexes. *Food Biophys.* **2006**, *1*, 51–56.
(11) Fishman, M. L.; Chau, H. K. Extraction of pectin by microwave heating under pressure. U.S. Patent 6,143,337, 2000.
(12) Fishman, M. L.; Chau, H. K.; Hoagland, P.; Ayyad, K. Characterization of pectin, flash extracted from orange albedo by microwave heating, under pressure. *Carbohydr. Res.* **2000**, *23*, 126–138.
(13) Fishman, M. L.; Cooke, P. H.; Coffin, D. R. Nanostructure of native pectin sugar acid gels visualized by atomic force microscopy. *Biomacromolecules* **2004**, *5*, 334–341.
(14) Kanchanasopa, M.; Manias, E.; Runt, J. Solid-state microstructure of poly(L-lactide) and L-lactide/meso-lactide random copolymers by atomic force microscopy (AFM). *Biomacromolecules* **2003**, *4*, 1203–1213.
(15) Fillisetti, T. M. C. C.; Carpita, N. C. Measurement of uronic acids without interference from neutral sugars. *Anal. Biochem.* **1991**, *197*, 157–162.
(16) Yoo, S.-H.; Fishman, M. L.; Savary, B.; Hotchkiss, A. T., Jr. Monovalent salt-induced gelation of enzymatically deesterified pectin. *J. Food Agric. Chem.* **2003**, *51*, 7410–7417.

(17) Voragen, A. G. J.; Schols, H. A.; Pilnik, W. Determination of the degree of methylation and acetylation of pectins by HPLC. *Food Hydrocolloids* **1986**, *1*, 65–70.
(18) Dubois, M.; Gilles, K. A.; Hamilton, J. A.; Rebers, P. A.; Smith, F. Colorimetric method for determination of sugars and related substances. *Anal. Chem.* **1956**, *28*, 350–356.
(19) AOAC Method 990.03.
(20) AACC Method 46-30.
(21) AOAC Method 22.052.
(22) Fishman, M. L.; Chau, H. K.; Kolpak, F.; Brady, J. Solvent effects on the molecular properties of pectins. *J. Agric. Food Chem.* **2001**, *49*, 4494–4501.
(23) Fishman, M. L.; Chau, H. K.; Coffin, D. R.; Hotchkiss Jr., A. T. A comparison of lime and orange pectin which were rapidly extracted from albedo. In *Advances in Pectin and Pectinase Research*; Voragen, F., Schols, H., Visser, R., Eds.; Kluwer Academic Publishers: Dordrecht, The Netherlands, 2003; pp 107–122.
(24) Fishman, M. L.; Chau, H. K.; Hoagland, P. D.; Hotchkiss, A. T. Microwave-assisted extraction of lime pectin. *Food Hydrocolloids* **2006**, *20*, 1170–1177.
(25) Fishman, M. L.; Cooke, P.; Levaj, B.; Gillespie, D. T. Pectin microgels and their subunit structure. *Arch. Biochem. Biophys.* **1992**, *294*, 253–260.
(26) Fishman, M. L.; Cooke, P.; Hotchkiss, A.; Damert, W. Progressive dissociation of pectin. *Carbohydr. Res.* **1993**, *248*, 303–316.
(27) Fishman, M. L.; Cooke, P. H.; Chau, H. K.; Coffin, D. R.; Hotchkiss, A. Global structures of high methoxyl pectin from solution and in gels. *Biomacromolecules* **2007**, *8*, 573–578.

Received for review August 31, 2007. Revised manuscript received December 5, 2007. Accepted December 13, 2007.

JF072600O